Cancer Research

Twist1 Regulates Vimentin through Cul2 Circular RNA to Promote EMT in Hepatocellular Carcinoma

Jing Meng[1], Shuang Chen[2], Jing-Xia Han[1], Baoxin Qian[3], Xiao-Rui Wang[4], Wei-Long Zhong[1], Yuan Qin[1], Heng Zhang[1], Wan-Feng Gao[1,2], Yue-Yang Lei[1,2], Wei Yang[2], Lan Yang[2], Chao Zhang[1,2], Hui-Juan Liu[2,4], Yan-Rong Liu[2], Hong-Gang Zhou[1], Tao Sun[1,2], and Cheng Yang[1,2]

Abstract

Twist is a critical epithelial–mesenchymal transition (EMT)–inducing transcription factor that increases expression of vimentin. How Twist1 regulates this expression remains unclear. Here, we report that Twist1 regulates Cullin2 (Cul2) circular RNA to increase expression of vimentin in EMT. Twist1 bound the Cul2 promoter to activate its transcription and to selectively promote expression of Cul2 circular RNA (circ-10720), but not mRNA. circ-10720 positively correlated with Twist1, tumor malignance, and poor prognosis in hepatocellular carcinoma (HCC). Twist1 promoted vimentin expression by increasing levels of circ-10720, which can absorb miRNAs that target vimentin. circ-10720 knockdown counteracted the tumor-promoting activity of Twist1 *in vitro* and in patient-derived xenograft and diethylnitrosamine-induced TetOn-Twist1 transgenic mouse HCC models. These data unveil a mechanism by which Twist1 regulates vimentin during EMT. They also provide potential therapeutic targets for HCC treatment and provide new insight for circular RNA (circRNA)-based diagnostic and therapeutic strategies.

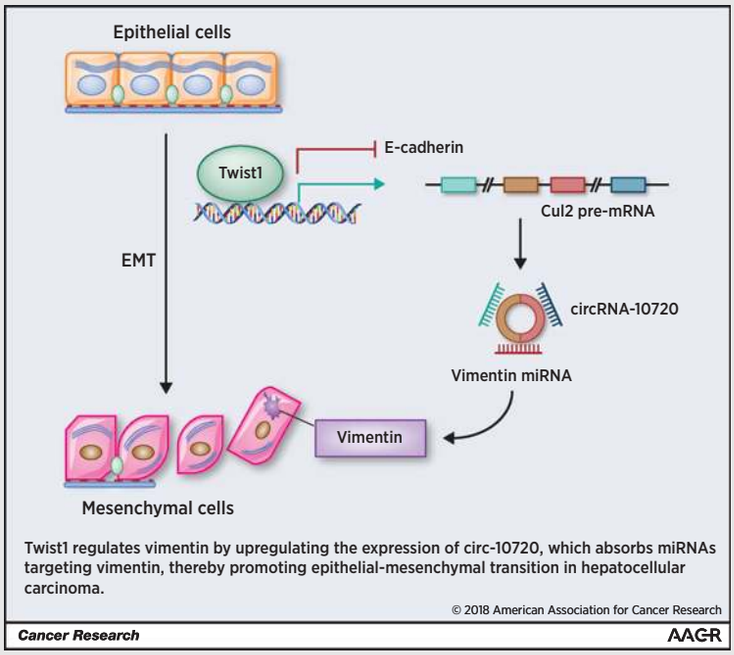

Significance: A circRNA-based mechanism drives Twist1-mediated regulation of vimentin during EMT and provides potential therapeutic targets for treatment of HCC.

Graphical Abstract: http://cancerres.aacrjournals.org/content/canres/78/15/4150/F1.large.jpg. *Cancer Res; 78(15); 4150–62. ©2018 AACR.*

Introduction

Epithelial–mesenchymal transition (EMT) is essential for tumor metastasis (1, 2) and involves a cellular reprogramming process in which epithelial cells dramatically alter their shape, exhibit increased motility and acquire a mesenchymal phenotype (3–5). Twist1 is one of the EMT-inducing transcription factors, which govern the transcription of EMT-associated genes via promoter activation or repression, downregulating the epithelial

[1]State Key Laboratory of Medicinal Chemical Biology and College of Pharmacy, Nankai University, Tianjin, China. [2]Tianjin Key Laboratory of Molecular Drug Research, Tianjin International Joint Academy of Biomedicine, Tianjin, China. [3]Department of Gastroenterology and Hepatology, Tianjin Key Laboratory of Artificial Cells, Tianjin Institute of Hepatobiliary Disease, Tianjin Third Central Hospital, Tianjin, China. [4]College of Life Science, Nankai University, Tianjin, China.

Note: Supplementary data for this article are available at Cancer Research Online (http://cancerres.aacrjournals.org/).

J. Meng, S. Chen, J.-X. Han, and B. Qian contributed equally to this article.

Corresponding Authors: Tao Sun and Cheng Yang, Nankai University, Haihe River Education Park, 38 Tongyan Road, Tianjin 300450, China. Phone: 8613-5129-22691; Fax: 022-6537-8009; E-mail: tao.sun@nankai.edu.cn; cheng.yang@nankai.edu.cn

doi: 10.1158/0008-5472.CAN-17-3009

phenotype-related genes, such as E-cadherin, and upregulating the mesenchymal cell phenotype-related genes, such as vimentin (6). Vimentin is a type 3 intermediate filament protein that is a critical EMT mesenchymal cell marker. Vimentin drives cell plasticity (7, 8) and is associated with poor prognosis and high frequency of metastasis (5, 9, 10). So far, several cis-elements and associated factors were reported to be required to regulate vimentin expression (11). For example, Sp1/Sp3 binds GC-Box 1 (12), Stat1/Stat3 bind the ASE (13, 14) and c-Jun can form either homo- or heterodimers with other AP-1 family members and bind the AP-1 sites (15), all of which can increase vimentin transcription. In addition, phosphorylated Slug does not directly bind the vimentin promoter, but it is likely to recruit additional transcription factors to upregulate vimentin (16). There is evidence that Twist1 upregulates vimentin expression in EMT (17), but the regulatory mechanism remains unclear, and there is no definitive Twist1-binding site on the vimentin promoter.

Cullin2 (Cul2) is a core component of multiple ECS (ElonginB/C-CUL2/5-SOCS-box protein) E3 ubiquitin–protein ligase complexes, which mediate the ubiquitination of target proteins. Cul2 was predicted to be a tumor-suppressor protein that degrades ubiquitinated HIFα (18, 19). However, it has also been reported that Cul2 is required for normal vasculogenesis and is involved in cell-cycle regulation (20). In recent years, circular RNAs (circRNA) have been identified as important molecules in gene-expression regulation at the post-transcriptional level (21). circRNAs result from a noncanonical form of alternative splicing, most commonly in which the splice donor site of one exon is ligated to the splice acceptor site of an upstream exon (22–24). There is evidence that some circRNAs might regulate miRNA functions, and roles in transcriptional control have also been suggested (25, 26). circRNAs were reported to function in gene regulation by competing with linear splicing (27). However, the role of Cul2 and its circRNA in tumor progression is poorly understood

In this study, we demonstrate that Twist1 promotes Cul2 transcription through binding to the *Cul2* promoter and upregulates Cul2 circRNA expression but represses *Cul2* expression. We next demonstrated that circ-10720 was positively correlated with Twist1 and promoted EMT progression. circ-10720 upregulated vimentin expression by adsorbing a series of miRNAs targeting vimentin. We further showed that circ-10720 knockdown blocked the promotive effect on vimentin in Twist1-overexpressing HCC cells and *in vivo*. This study describes a novel Twist1–circRNA–vimentin regulation mechanism and provides a potential therapeutic target for mesenchymal tumors.

Materials and Methods

Cell culture and plasmid transfection

PLC-PRF-5 and SMMC-7721 cells were cultured in RPMI-1640 medium (HyClone), and HEK-293T cells were cultured in DMEM (HyClone) supplemented with 10% (v/v) fetal bovine serum (Thermo Fisher Scientific) at 37 °C in humidified atmosphere containing 5% CO_2. The PLC-PRF-5, SMMC-7721, and HEK-293T cell lines were used within approximately 35, 42, and 24 passages of thawing original stocks, respectively, and tested for *Mycoplasma* before use. All cells were purchased from KeyGen Biotech (Nanjing, China) and the company provides complete cell identification. All the cells periodically authenticated by morphologic inspection and biomarkers detection of hepatocellular carcinoma, growth curve analysis, and *Mycoplasma* testing. The plasmid information is provided in Supplementary Table S1 of the Supplementary Data. The cloning primers and circ-10720 siRNA are provided in Supplementary Table S2. siRNA, miRNA mimic and mutant miRNAs were synthesized by Genepharma. All the plasmids or miRNA mimic were transfected into cells using Lipofectamine 2000 (Invitrogen) or nanoparticle (Micropoly Biotech) transfection reagents. The lentiviral vector pLCDH-ciR carrying circ-10720 and two assistant vectors-psPAX2, pMD2.G were transiently transfected into HEK293T cells. Viral supernatants were collected 48 hours later, clarified by filtration and concentrated by ultracentrifugation.

qRT-PCR

Total RNA was isolated using TRIzol reagent (Invitrogen). cDNA synthesis was performed with Oligo(dT), random or miRNA-specific stem-loop primers using a Quantscript RT Kit (Tiangen). A SYBR RT-PCR kit (Tiangen) was used for transcript quantification with specific primers. The expression levels were quantified using the $2^{-\Delta\Delta C_t}$ method, with U6 or β-actin as the internal control. The primers were provided in Supplementary Table S3 of the Supplementary Data.

Dual-luciferase reporter gene assay

The recombinant luciferase reporter plasmids contained *Cul2* promoter (pEZX-PG04-Cul2) and the potential miRNA-binding site sequences of the vimentin 3′-untranslated region (UTR; psiCHEK-2-vimentin-3′UTR) and circ-10720 (psiCHEK-2-circ-10720). *Cul2* promoter and Twist1 overexpressed or knockdown vectors cotransfected into PLC-PRF-5 or SMMC-7721 cells, respectively. After 48 hours of transfection, gaussia luciferase and secreted alkaline phosphatase were measured by dual-luciferase reporter gene assay kit (GeneCopoeia). HEK293T cells were transfected with *vimentin* 3′-UTR and circ-10720 luciferase reporter vector and miRNA mimics. *Renilla* luciferase acted as an internal control to normalize transfection efficiencies. After 48 hours of transfection, luciferase activities were detected with a dual-luciferase reporter gene assay kit according to the manufacturer's instructions.

Cell invasion assays

Cell invasion assay was performed using a 24-well Transwell chamber. At 48 hours after transfection, PLC-PFR-5 and SMMC-7721 cells were trypsinized and transferred to the Matrigel-coated top chamber containing 100 μL of serum-free medium. FBS was added to the bottom chamber as chemoattractant. After 24 hours, cells on the bottom of the chambers were fixed in 4% paraformaldehyde and stained with 0.1% crystal violet. Cells that invaded into the bottom surface were counted in at least five random fields (magnification, ×200; Nikon). Each experiment was performed in triplicate.

Wound-healing assay

Twenty-four hours after transfection, a straight scratch was created in the center of each well using a micropipette tip. Cell migration was assessed by measuring the movement of the cells into the scratch in the well. The wound-closure speed after 24 and 48 hours was determined and normalized to the length at 0 hours. Each experiment was performed in triplicate.

Immunofluorescence

PLC-PRF-5 and SMMC-7721 cells were fixed with 3.7% formaldehyde in PBS for 5 minutes at room temperature and blocked with 1% BSA for 30 minutes. The cells were incubated overnight at 4°C with vimentin antibody (1:200, Affinity), E-cadherin antibody (1:200, Affinity) and then incubated with FITC- and TRITC-labeled secondary antibodies (1:200, Earthox LLC) for 1 hours at room temperature. Each step was followed by two 5-minute washes in PBS. The prepared specimens were counterstained with DAPI (Southern Biotechnology Associates) for 2 minutes and observed with a confocal microscope (Nikon).

Chromatin immunoprecipitation assay

Chromatin immunoprecipitation sequencing (ChIP-seq) experiments were performed using 1×10^7 SMMC-7721 cells. Cells were cross-linked in 1% formaldehyde (EM grade; Thermo Scientific) for 10 minutes, quenched with 0.25 mol/L glycine and washed in cold PBS. The cell pellet was resuspended in 1 mL of Cell Lysis Buffer containing 1 × Protease Inhibitor Cocktail II, incubated in ice for 15 minutes, dissociated by pipetting and pelleted by centrifugation at 800 × *g* for 5 minutes at 4 °C. The pellet was resuspended in 1 mL of Nuclear Lysis Buffer. Effective sonication was confirmed by Bioanalyzer analysis. The chromatin fraction was incubated with an anti-Twist1 mAb (1:100, Abcam) overnight at 4 °C. The protein/DNA complexes were reversed cross-links to obtain free DNA. The DNA was purified using spin columns, and the samples were sequenced by Genergy Biotechnology.

Western blotting

Cells were washed with PBS and lysed in ice-cold lysis buffer with protease Inhibitor Cocktail (Sigma) on ice for 30 minutes. Lysates were separated by electrophoresis and transferred onto polyvinylidene difluoride membranes (Millipore). The membranes were blocked and incubated with primary antibody against Cullin2 (1:1,000, Affinity), Twist1(1:1,000, Affinity), vimentin (1:1,000, Affinity), and GAPDH (1:5,000, Affinity) in 4°C overnight and then incubated with a horseradish peroxidase–conjugated goat anti-rabbit IgG secondary antibody (Thermo-Scientific) for 1 hour at room temperature. Protein expression was assessed using enhanced chemiluminescent substrate (Millipore) and exposure to chemiluminescent film.

Patient-derived xenograft model

Fresh surgical HCC tumor tissues (F0) were collected immediately after surgery from S.G. Hospital (Shandong, China), Medical General Hospital of Tianjin, Tumor Hospital of Tianjin and the Hospital of Shunyi District, Beijing. According to the Declaration of Helsinki, studies were performed after approval of the ethics committee of Nankai University, including the use of animal experiments and tumor specimens. Written informed consent was obtained from each patient. The patient information was shown in Supplementary Table S4. According to Twist1 expression detected by qRT-PCR, eight Twist1-Low expression tumor tissues and eight Twist1-High tissues were selected. Then, the tumors were divided into 2 groups (Twist1-Low group, Twist1-High, group) and cut into 1 to 2 mm^3 pieces and placed in antibiotic-containing RPMI medium. Tumor fragments were subcutaneously implanted into pockets made in each side of the lower back of SCID mice. When the tumor size reached 100 to 200 mm^3, the samples (called F1) were divided into pieces for *in vivo* passaging to construct F2 tumors and then F3 constructed as described above (28). When the F3 tumor size reached 100 to 200 mm^3, 1×10^7 TU lentiviral particles carrying circ-10720 in HBSS was intratumorally injected into Twist1-Low groups (Twist1-Low+circ-10720 groups) and HBSS group as control (Twist1-Low+control group); 10 OD circ-10720 siRNA was intratumorally injected into Twist1-High groups (Twist1-High+circ-10720 siRNA groups) and control siRNA injection as control (Twist1-High+control siRNA group). Each group had four mice, which were injected every 3 days for 18 days. Serum α-fetoprotein (AFP) level was detected using ELISAs (Autobio, China). Tumor diameters were serially measured with a digital caliper every 3 days, and tumor volumes were calculated using the following formula: $V = (L \times W^2)/2$, where V, volume; L, length; and W, width. On day 24, mice were euthanized, and tumor tissues were collected, fixed with 10% formalin, and embedded in paraffin. The remaining tumor tissues were maintained in a −80 °C deep freezer for RNA isolation. All animal experiments were performed under approved protocols of the institutional animal use and care committee.

Diethylnitrosamine-induced TetOn-Twist1 mouse HCC model

Teton-Twist1 mice were generated using a site-specific single-copy integration strategy (29, 30). Fourteen- to 15-day-old mice were injected with diethylnitrosamine (DEN; 20 mg/kg body weight; Sigma) to initiate tumor growth. After 2 weeks, the mice were injected with the phenobarbital-like inducer TCPOBOP (3 mg/kg body weight; Sigma) once every 2 weeks for a total of seven times to promote tumor growth (31, 32). At the end of treatment, all mice that developed HCC were randomly divided into two groups. One group of six mice received no doxycycline in the drinking water (control group), and the second group of 12 mice received doxycycline (Twist1 group). After 7 days of doxycycline treatment, half of the mice in the Twist1 group were treated with si-circ-10720 (10 OD) via intravenous injection, and the other half were treated with siRNA control. Two weeks later, the mice were euthanized, and the liver tissues were evaluated to determine tumor number and then fixed with 10% formalin and embedded in paraffin. All animal experiments were performed under approved protocols of the Institutional Animal Use and Care Committee.

IHC assay and analysis

The tissues were incubated with xylene for deparaffinization and decreasing concentrations of ethanol for rehydration. Next, 3% hydrogen peroxide was applied to block endogenous peroxidase activity. The microwave antigen retrieval technique was used for antigen retrieval. After being blocked, the samples were incubated with the following primary antibodies overnight at 4°C: Twist1 (1:200, Affinity), E-cadherin (1:200, Affinity), and vimentin (1:200, Affinity) antibody. PBS displaced the primary antibody in the negative group. The secondary antibody was subsequently added using an horseradish peroxidase–polymer anti-mouse/rabbit IHC kit (Maixin Biotech) for 1 hour at room temperature. Then, the samples were developed with diaminobenzidine reagent, counterstained with hematoxylin and mounted with permount (33). The immunohistochemistry score was calculated by multiplying the intensity (0 = negative, 1 = canary yellow, 2 = claybank, 3 = brown) and the positive cell percentage scores (1 = less than 25%, 2 = 25% to 50%, 3 = 51% to 75%, 4 = more than 75%).

FISH

HCC tissue microarrays containing 381 cases were purchased from US Biomax for IHC and FISH. The circ-10720, circ-31603, circ-12201, circ-21832, circ-20827, and circ-31230 expression levels in tissues were evaluated with FISH using a specific FAM-labeled locked nucleic acid-modified oligonucleotide circRNA probe (GenePharma) on the tissue arrays. A quantitative scanning approach was used to evaluate the staining and expression of circ-10720 with confocal laser scanning microscopy (Eclipse Ti, Nikon, Japan). The circRNA probe sequences for FISH are listed in Supplementary Table S5 of the Supplementary Data.

Scanning electron microscopy

Cells were grown on climbing films and transfected with circ-10720 or si circ-10720. After 48 hours, cells were fixed and dehydrated in acetone/isoamyl acetate (1:1) and dried with a gradient concentration of acetonitrile. After being coated with gold, the cells were photographed using a scanning electron microscope (JEOL 6000, Japan).

Statistical analysis

Statistical analyses were performed using GraphPad Prism 6 and SPSS v. 19. Statistically significant differences were calculated using Student *t* test, one-way ANOVA, Pearson's correlation, χ^2, and Kaplan–Meier, as appropriate. Values of $P < 0.05$ were considered significant.

Results

circ-10720 expression in clinical HCC tissues is associated with metastasis and prognosis of patients

To explore the transcriptional regulation of Twist1, we analyzed the genome-wide transcriptional Twist1 targets. ChIP-based deep sequencing (ChIP-seq) was performed in SMMC-7721 cells using antibodies against Twist1. We analyzed the genomic signatures of Twist1, revealing the binding motifs of Twist1 on the *Cul2* and its promoter, which are listed in Fig. 1A and the ChIP-seq date binding peak are shown in Supplementary Fig. S1A–S1C. ChIP-PCR analysis of SMMC-7721 cells using specific antibodies against Twist1 showed occupancy of Twist1 on the *Cul2* promoter, validating the ChIP-seq results (Fig. 1B). The findings demonstrated that Twist1 directly binds to the *Cul2* promoter. Furthermore, we used a dual-luciferase reporter system to detect the effect of Twist1 on the activity of the *Cul2* promoter. The results showed that Twist1 overexpression increased *Cul2* promoter activity and that Twist1 knockdown decreased Cul2 promoter activity (Fig. 1C).

To investigate the Cul2 expression profile in HCC tissues and the effect on HCC malignancy, we analyzed 75 HCC tissue samples. Although Twist1 regulated *Cul2* promoter activity, there was no significant difference in the expression of Cul2 in metastatic and nonmetastatic HCC tissues ($P = 0.489$; Fig. 1D). Therefore, we hypothesized that the circRNA generated from Cul2 may play an important role in HCC development. We predicted several circRNAs on the circRNADb. Next, we examined the expression of 7 circRNAs in metastatic and non-metastatic HCC tissues. Among them, we found that circ-10720 expression was consistently and significantly increased in metastatic HCC compared with that in non-metastatic HCC ($P = 0.011$; Fig. 1E). Thus, in this study, we focused on the expression and role of circ-10720 in HCC progression. The circ-10720 expression level increased along with the progression of clinical stage and pathology grade in 381 HCC tissues (Fig. 1F). Furthermore, we detected circ-10720 expression in different groups of HCC tumor tissues. The expression of circ-10720 was increased in AFP-positive (AF*P* > 400 ng/mL) and $HBsAg^+/HBeAb^+/HBcAb^+$ groups. The results showed that circ-10720 expression was also associated with AFP ($P = 0.001$) and hepatitis B markers ($P = 0.038$; Fig. 1G). In addition, we examined the relationship between circ-10720 expression and a number of other factors, such as age, sex, smoking, drinking, carbohydrate antigen (CA-199, CA-125), enzymes related to liver function, and so on. The results showed that there was no significant association between circ-10720 expression and these parameters in HCC (Supplementary Fig. S2A–S2C). In summary, upregulation of circ-10720 suggested a link with aggressive characteristics of HCC.

Further statistical analysis showed that the expression levels of circ-10720 and Twist1 in HCC tumor tissues were positively related ($r = 0.425$, $P = 0.0001$; Fig. 1H). Furthermore, we demonstrated an association between survival time and the expression of circ-10720 and Twist1 in patients with HCC. The Kaplan–Meier survival curve revealed that elevated circ-10720 expression indicated poor survival in patients with HCC (Fig. 1I). Concurrent high circ-10720 and Twist1 expression was associated with shorter overall survival, and the median survival time dropped from 32 months to 28.5 months (Fig. 1J). These results demonstrated that the expression levels of Twist1 and circRNA are not entirely consistent in HCC, and Twist1 may also affect survival time by regulating other proteins or circRNAs in patients with HCC.

circ-10720 regulated by Twist1 exhibits oncogenic effects in HCC cells.

To detect how Twist1 regulates Cul2 circRNA in HCC, we measured pre-mRNA, mRNA and circ-10720 of Cul2. The primer design sketch is shown in Fig. 2A. Twist1 overexpression increased pre-mRNA levels of Cul2 in PLC cells, and Twist1 knockdown decreased Cul2 pre-mRNA levels in SMMC-7721 cells (Fig. 2B). Moreover, the expression level of Cul2 mRNA and protein was decreased under Twist1 overexpression in PLC cells and increased under Twist1 knockdown in SMMC-7721 cells (Fig. 2C and D). Furthermore, we confirmed that endogenous expression of circ-10720 generated from Cul2. Cul2 is located in chromosome 10, and circ-10720 is generated from exon 6 to exon 12 (Fig. 2E). The expression of circ-10720 was increased in Twist1-overexpressing PLC cells and decreased in Twist1 knockdown SMMC-7721 cells (Fig. 2F).

To determine the function of circ-10720 in HCC cells, siRNA targeting the back-splice junction sequence of circ-10720 was designed (Fig. 2G, left). We found that siRNA targeting the back-splice junction knocked down only the circular transcript and did not affect the expression of linear species (Fig. 2G, right). The effect of circ-10720 on cell phenotype was observed using scanning electron microscopy. Cell pseudopodia were increased and the cell morphology converted to a mesenchymal phenotype in circ-10720–overexpressing PLC cells, whereas SMMC-7721 cells became epithelioid after circ-10720 depletion (Fig. 2H). EMT markers were analyzed in circ-10720 overexpression or knockdown cells using immunofluorescence. The results showed

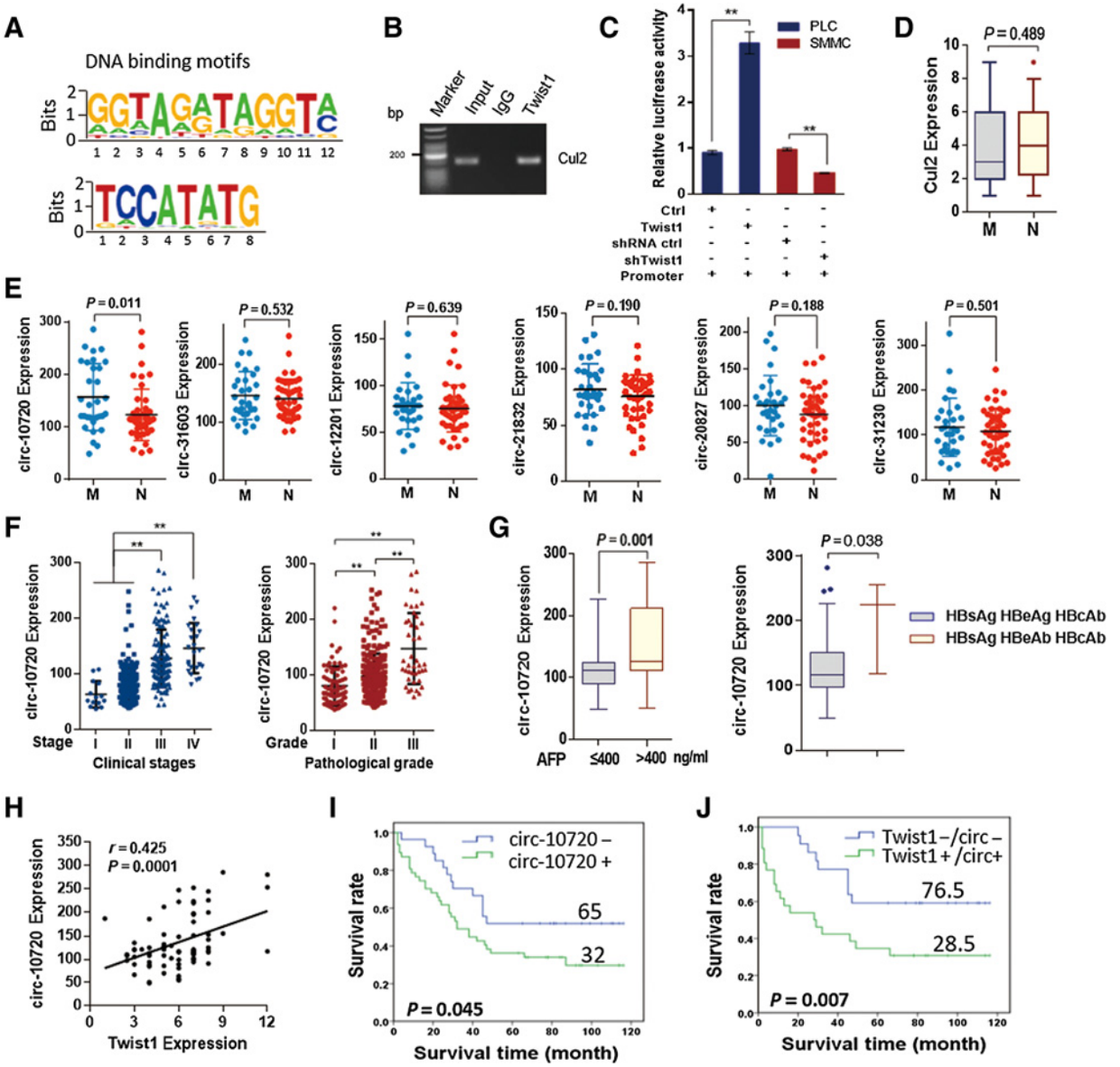

Figure 1.

circ-10720 expression in clinical HCC tissues is associated with metastasis and patient prognosis. **A,** ChIPseek analysis of the DNA-binding motifs of Twist1 on the promoters of Cul2. **B,** ChIP experiments on the *Cul2* promoter using antibodies against Twist1 in SMMC-7721 cells. **C,** After Cul2 reporter gene plasmid transfected into cells for 48 hours, luciferase activity was measured in PLC cells with Twist1 overexpression or in SMMC cells with Twist1 knockdown. Each bar represents the mean ± SD for biological triplicate experiments. **, $P < 0.01$, Student *t* test. **D,** Relative expression of Cul2 in 75 HCC tumor tissues measured via IHC. M, metastasis; N, no metastasis. Student *t* test. **E,** Relative expression of six Cul2 circRNAs in 75 HCC tumor tissues measured via FISH. *, $P < 0.05$, Student *t* test. **F,** Correlation between circ-10720 expression and clinical stage (I–IV; $P < 0.01$) and pathology grade (I–III; $P < 0.01$) in 381 cases of HCC tumor tissues. *, $P < 0.05$; **, $P < 0.01$, one-way ANOVA. **G,** The circ-10720 expression in different groups of HCC tumor tissues. AFP ≤ 400 ng/mL versus AF*P* > 400 ng/mL ($P = 0.001$), $HBsAg^+/HBeAg^+/HBcAb^+$ versus $HBsAg^+/HBeAb^+/HBcAb^+$ ($P = 0.038$). Student *t* test. **H,** Correlation analysis of tumor tissues from 75 HCC cases between circ-10720 and Twist1 expression ($P < 0.001$). **I,** Kaplan–Meier plots of the overall survival rate of 75 patients with HCC with circ-10720 low (blue) or high (green) expression levels ($P = 0.045$). **J,** Kaplan–Meier plots of overall survival rate of 75 patients with HCC with Twist1/circ-10720 low (blue) or high (green) levels ($P = 0.007$).

that E-cadherin expression was reduced and vimentin expression was increased in circ-10720–overexpressing PLC cells, and that was in contrast in circ-10720–silenced SMMC-7721 cells (Fig. 2I). Furthermore, we found that circ-10720 promoted proliferation, migration and invasion of PLC cells and circ-10720 knockdown inhibited cell migration and invasion (Fig. 2J and K). In sum, Twist1 promoted circ-10720 expression, and circ-10720 plays an oncogenic role in HCC cells.

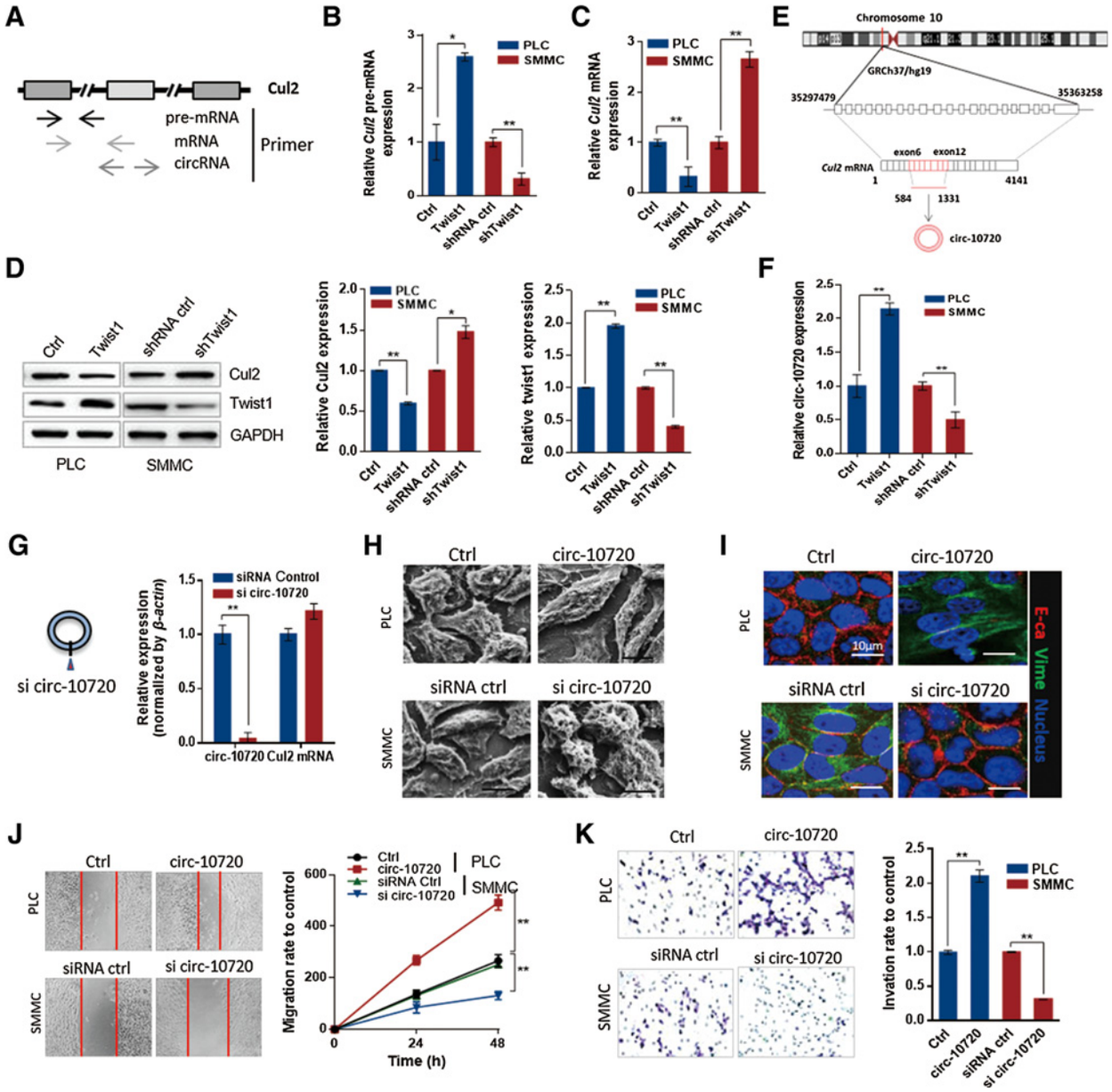

Figure 2.

circ-10720 regulated by Twist1 exhibits oncogenic effects in HCC cells. **A,** The strategy used to detect pre-mRNA, mRNA, and endogenous circRNA. **B,** qRT-PCR of *Cul2* pre-mRNA expression by overexpression or silencing of Twist1. **C,** qRT-PCR analysis of Cul2 mRNA levels in Twist1 overexpression or knockdown cells. **, $P < 0.01$, Student *t* test. **D,** Western blot analysis of Twist1 and Cul2 protein levels in Twist1 overexpression or knockdown cells. Intensity of each band from biological triplicate experiments was quantified by densitometry with the ImageJ software with GAPDH as a normalizer. *, $P < 0.05$; **, $P < 0.01$, Student *t* test. **E,** Relationship between *Cul2* genomic DNA, mRNA, and circRNA. **F,** qRT-PCR analysis of circ-10720 levels under Twist1 overexpression or knockdown. **, $P < 0.01$, Student *t* test. **G,** Schematic model of siRNA. si-circ-10720 targets the back-splice junction of circ-10720 (left). si-circ-10720 knocked down only the circular transcript and did not affect the expression of linear species (right). **, $P < 0.01$, Student *t* test. **H,** The morphologic changes under circ-10720 overexpression in PLC cells and knockdown in SMMC-7721 cells observed with scanning electron microscopy. **I,** Immunofluorescence analysis of E-cadherin and vimentin expression under circ-10720 overexpression in PLC cells or knockdown in SMMC-7721 cells. **J,** Migration of PLC and SMMC-7721 cells was detected after transfection with circ-10720 and si-circ-10720, respectively, for 24 and 48 hours. **, $P < 0.01$, Student *t* test. **K,** Cell invasion was determined with Matrigel-coated Transwell assays. The cells that crossed the Matrigel-coated filter were fixed, stained, and counted. **, $P < 0.01$, Student *t* test. All data are presented as the mean ± SD for biological triplicate experiments.

Twist1 upregulates vimentin expression by increasing circ-10720, which adsorbs miRNA.

To identify miRNAs that bind to circ-10720, we performed a context score percentile screening in the CircInteractome database. Fourteen miRNAs (miR-1246, miR-127-5p, miR-331-5p, miR-1200, miR-888, miR-587, miR-578, miR-656, miR-890, miR-490-5p, miR-1238, miR-548g, miR-513a-3p, and miR-521) among the 27 miRNAs with a context score percentile >90 were selected (Fig. 3A).

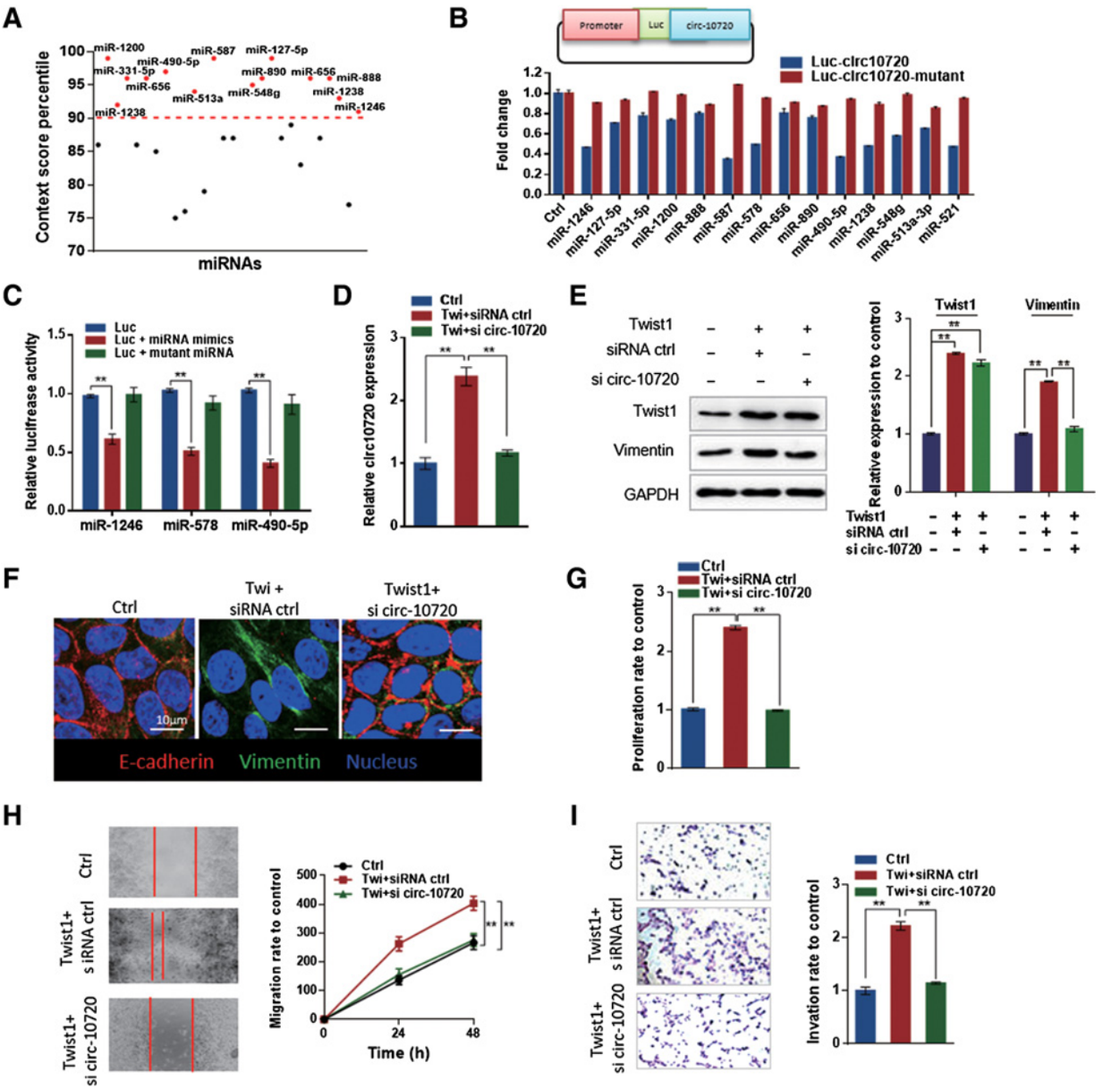

Figure 3.

Twist1 upregulates vimentin expression through increased circ-10720, which adsorbs miRNA. **A,** Context score percentile of 27 miRNAs that bind to the circ-10720 sequence. Fourteen miRNAs with a context score percentile >90 are indicated by red dots. **B,** The entire circ-10720 sequence (light blue) was cloned into the downstream region of the luciferase gene, denoted Luc-circ-10720. The luciferase activities of Luc-circ-10720 or Luc-circ-10720–mutant in HEK-293T cells cotransfected with miRNA mimic were measured with a luciferase reporter assay. **C,** The effect of miRNAs and their mutant fragments on the luciferase activity of the vimentin 3′-UTR was tested with a luciferase reporter assay. **, $P < 0.01$, one-way ANOVA. **D,** The expression level of circ-10720 was determined with qRT-PCR in PLC cells transfected with Twist1 alone or cotransfected with circ-10720 siRNA. **, $P < 0.01$, one-way ANOVA. **E,** The expression level of vimentin was measured by Western blot analysis in PLC cells transfected with Twist1 alone or cotransfected with circ-10720 siRNA. Intensity of each band from biological triplicate experiments was quantified by densitometry with the ImageJ software with GAPDH as a normalizer. **, $P < 0.01$, one-way ANOVA. **F,** Representative immunofluorescence images of E-cadherin and vimentin in PLC cells transfected with Twist1 alone or cotransfected with circ-10720 siRNA. **G,** The proliferation of PLC-PRF-5 cells transfected with Twist1 alone or cotransfected with circ-10720 siRNA. **, $P < 0.01$, one-way ANOVA. **H,** The migration of PLC cells transfected with Twist1 alone or cotransfected with circ-10720 siRNA assessed with wound-healing assays. **, $P < 0.01$, one-way ANOVA. **I,** Cell invasion assays were performed in PLC cells transfected with Twist1 alone or cotransfected with circ-10720 siRNA. **, $P < 0.01$, one-way ANOVA. All data are presented as the mean ± SD for biological triplicate experiments.

We further mutated each miRNA target site from the luciferase reporters with inclusion of the circ-10720 sequence in the 3′-UTR and circ-10720–expressing vector (Supplementary Fig. S3A). We found that transfection with the miRNAs had no significant effect on luciferase activity when the corresponding target sites were mutated in the luciferase reporter (Fig. 3B). The result suggested that circ-10720 may function as a sponge to these miRNAs. Among them, miR-1246, miR-578 and miR-490-5p were predicted by the miRNA database to target vimentin (Supplementary Fig. S3B). In addition, we analyzed the expression level of the three miRNAs in human normal live tissues and HCC tissues in TCGA database (Supplementary Fig. S3C). MiR-1246, miR-578, and miR-490-5p are indeed expressed in human HCC samples. The expression of miR-490-5p in HCC is higher than that of miR-1246 and miR-578. A luciferase reporter assay revealed that miRNAs inhibited the luciferase activities of the *vimentin* 3′-UTR, but mutant miRNA mimics abrogated the suppressive effect (Fig. 3C). The inhibition of miR-490-5p was stronger than miR-1246 and miR-578. Therefore, maybe miR-490-5p is the major miRNA regulating vimentin in HCC because of its high expression and inhibitory effects to *vimentin* 3′-UTR activities.

To detect the target genes based on the miRNA predictions targeted vimentin for circ-10720 adsorption, we conducted the gene-expression profiling and proteomic analysis in HCC cells overexpressed circ-10720. Gene set enrichment analysis (GSEA) was used to identify gene sets that exhibited significant overlaps with those gene differences between control and circ-10720–overexpressed PLC-PRF-5 cells. Gene ontology analysis was used to analyze the differential gene of biological processes, molecular function and cellular component in PLC-PRF-5 cells under circ-10720 overexpression treatment. As shown in Supplementary Fig. S4A, cells overexpressed with circ-10720 were enriched in gene sets associated with cancer, EMT, and VEGF signaling pathways, and cell adhesion–related pathways were downregulated. In GO analysis, intracellular signal introduction, wound healing, growth factor activity, and so on were upregulated (Supplementary Fig. S4B). Some of the upregulated genes are shown in Supplementary Fig. S4C. The GSEA (Supplementary Fig. S5A) and GO analysis (Supplementary Fig. S5B) results of proteomic data are similar to those of the gene-expression profiling analysis. The detailed upregulated genes associated with intracellular transport, cellular invadopodia-related proteins, multicellular organism growth, TGFβ receptor signaling pathways and so on are shown in Supplementary Fig. S5C.

To examine whether Twist-mediated vimentin regulation occurs through circRNA, we performed loss-of-function assays. circ-10720 expression was markedly increased in PLC cells overexpressing Twist1, and knockdown of circ-10720 in Twist1-overexpressing cells offset the increase in circ-10720 (Fig. 3D). In HCC, Twist1 was positive correlated with vimentin and co-expression of the two proteins presented a shorter survival time (Supplementary Fig. S6A–S6B). In addition, Western blotting results showed that Twist1 enhanced vimentin expression levels, while circ-10720 knockdown in Twist1-overexpressing PLC cells offset the promotive effect of Twist1 on vimentin expression (Fig. 3E). Immunofluorescence analysis showed that the E-cadherin expression level significantly decreased and the vimentin expression level increased when Twist1 was overexpressed. circ-10720 knockdown in Twist1-overexpressing PLC cells blocked the influence of Twist1 on E-cadherin and vimentin expression (Fig. 3F). Furthermore, circ-10720 knockdown offset the enhanced cell proliferation (Fig. 3G), migration (Fig. 3H) and invasion (Fig. 3I) induced by Twist1 overexpression. The above results suggest that Twist1 promoted vimentin expression and HCC malignancy through circ-10720 adsorbing miRNAs, which target vimentin.

Intratumoral silencing of circ-10720 blocks the promotive effect of Twist1 mediated on vimentin expression in a patient-derived xenograft model of HCC.

To investigate Twist1 regulation of vimentin expression via circ-10720 *in vivo* and the function of circ-10720 *in vivo*, we established a patient-derived xenograft model (Fig. 4A). Twist1 expression levels in tumor tissues from patients with HCC were detected using qRT-PCR, and the tissues selected were assigned to two groups, Twist1-Low and Twist-High groups (Fig. 4B). Mice were implanted with different types of tumor tissues, half of the mice in the Twist1-Low group were intratumorally injected with lentiviral particles carrying circ-10720 and half of the mice in the Twist1-High group were intratumorally injected with si-circ-10720 when the tumor volume reached 100 to 200 mm^3. High Twist1 expression levels can significantly promote the growth of tumors. Overexpression of circ-10720 in Twist1-Low tumors increased tumor volumes. Knockdown of circ-10720 in Twist1-High tumors blocked the promoting effect of Twist1 on tumor growth (Fig. 4C). The expression levels of circ-10720 were detected in tumors of Twist1-Low+control, Twist1-Low+circ-10720, Twist-High+siRNA control, and Twist-High+si-circ-10720 groups using qRT-PCR. The results showed that the circ-10720 expression level was higher in the Twist1-Low+circ-10720 and Twist-High+siRNA control group than that in the Twist-Low+control group, and knockdown of circ-10720 neutralized the promotion in Twist1-High tumors (Fig. 4D). High Twist1 expression levels significantly increased vimentin expression levels, but circ-10720 knockdown counteracted the promotive effect of Twist1 on vimentin expression. Overexpression of circ-10720 increased the vimentin expression. Knockdown circ-10720 in Twist1-High groups and overexpression of circ-10720 in Twist-Low group had no obvious effect on Twist1 expression levels (Fig. 4E and F). Furthermore, we analyzed the correlation between Twist1, vimentin and circ-10720 expression in tumors. The results showed that the Twist1, circ-10720 and vimentin expression levels were positively related in tumor tissues (Fig. 4G). The serum AFP expression levels were consistent with those of circ-10720 in the four groups (Fig. 4H). Thus, these results demonstrate that overexpression of circ-10720 increased tumor growth and vimentin expression; circ-10720 knockdown blocked the promotive effect of Twist1 on vimentin and HCC progression *in vivo*.

Silencing of circ-10720 suppresses Twist1-induced tumor metastasis in a DEN-induced TetOn-Twist1 mouse HCC model

To demonstrate the influence of circ-10720 knockdown on Twist1-induced metastasis, we employed a DEN-induced TetOn-Twist1 transgenic mouse HCC model (29, 30). To generate HCC, TetOn-Twist1 mice were treated with DEN to initiate tumor growth, followed by administration of TCPOBOP every 2 weeks for a total of seven times to promote tumor growth (32). At the end of the treatment, all the mice that developed HCC were randomly divided into two groups. One group received no doxycycline in the drinking water (control group), and the second group received doxycycline to allow continuous Twist1

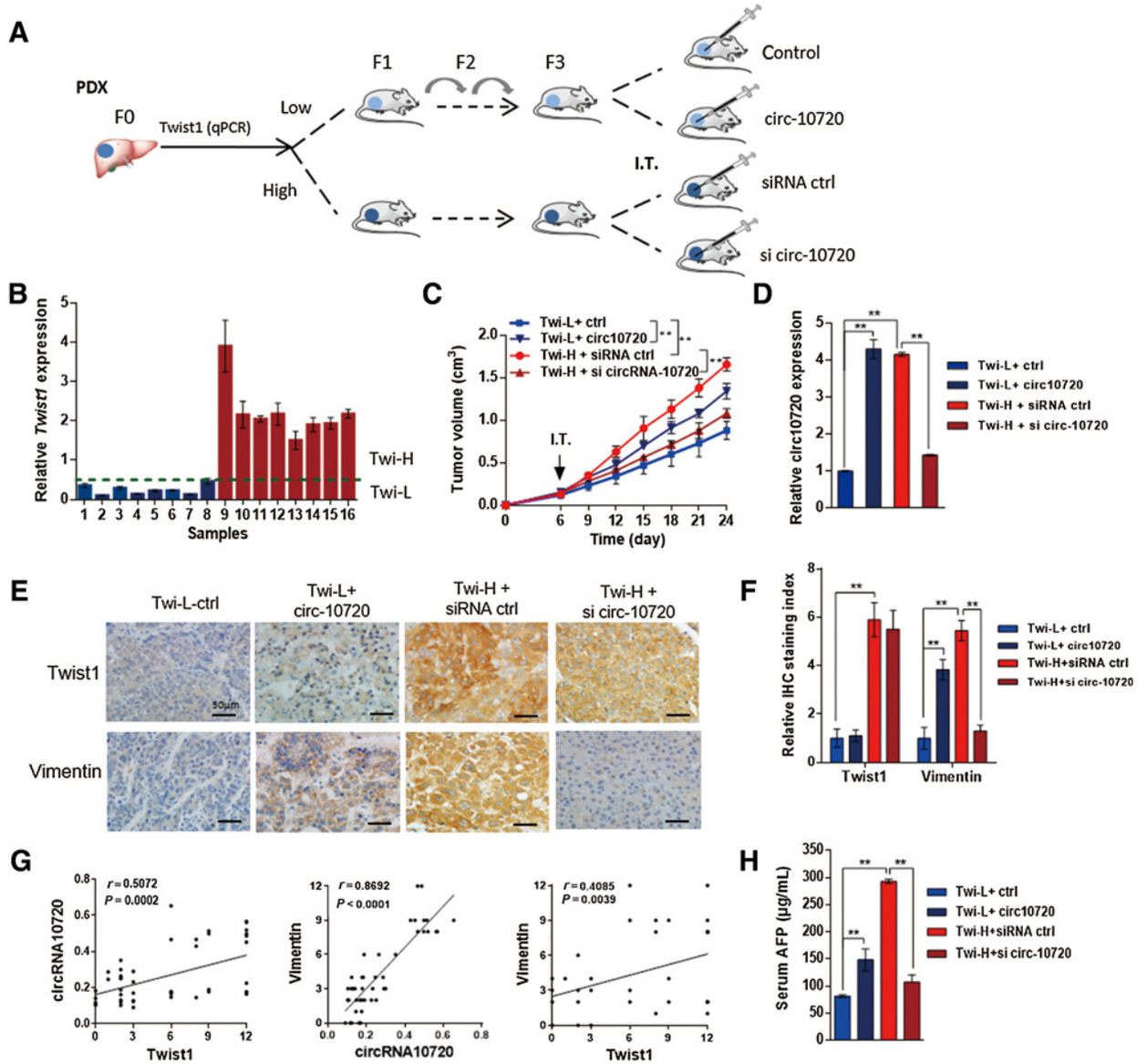

Figure 4.

Intratumoral silencing of circ-10720 blocks the promotive effect of Twist1 mediated on vimentin expression in a patient-derived xenograft (PDX) model of HCC. **A,** Schematic of intratumoral circ-10720 or silencing of circ-10720 in the PDX model. **B,** Twist1 expression levels in 16 fresh HCC tumor samples were measured with qRT-PCR, and the tumor samples were divided into two groups, namely, Twist1-Low (Twi-L) and Twist1-High (Twi-H) groups. **C,** Tumor growth curve of Twi-L + control, Twi-L + circ-10720, Twi-H + siRNA control, and Twi-H + si-circ-10720 groups. Tumor volume was monitored every 3 days for 24 days. Each point represents the mean ± SD for different animal measurements ($n = 4$). *, $P < 0.05$; **, $P < 0.01$, one-way ANOVA. **D,** qRT-PCR analysis of circ-10720 levels in tumor tissues of Twi-L + control, Twi-L + circ-10720, Twi-H + siRNA control, and Twi-H + si-circ-10720 groups. Each bar represents the mean ± SD for triplicate measurements of four xenografts in each group. **, $P < 0.01$, one-way ANOVA. **E** and **F,** Twist1 and vimentin expression in the tumor tissues of Twi-L + control, Twi-L + circ-10720, Twi-H + siRNA control, and Twi-H + si-circ-10720 groups were analyzed via IHC. Each bar represents the mean ± SD for triplicate measurements of four xenografts in each group. **, $P < 0.01$, one-way ANOVA. **G,** Correlation analysis between Twist1 and circ-10720 ($P = 0.0002$), circ-10720 and vimentin ($P < 0.0001$), and Twist1 and vimentin ($P = 0.0039$). The points represent the triplicate measurements of four xenografts in every group. **H,** AFP was detected by ELISA after intratumoral injection of circ-10720 and si-circ-10720 for 18 days. **, $P < 0.01$, one-way ANOVA. Each bar represents the mean ± SD for triplicate measurements of four xenografts in each group.

expression (Twist group). After 7 days of doxycycline treatment, half of the mice in the Twist1 group were treated with si-circ-10720 via intravenous injection (Twi + si-circ-10720 group), and the other half were treated with siRNA control (Twi + siRNA ctrl group; Fig. 5A).

Human *Cul2* is located in chromosome 10, and murine *Cul2* is located in chromosome 18. Analysis using the basic local alignment search tool indicates 91% identity of Cul2 mRNA sequences between human and murine. Human circ-10720 is generated from exon 6 to exon 12 (Fig. 2E). The exons 6-12 of the mouse

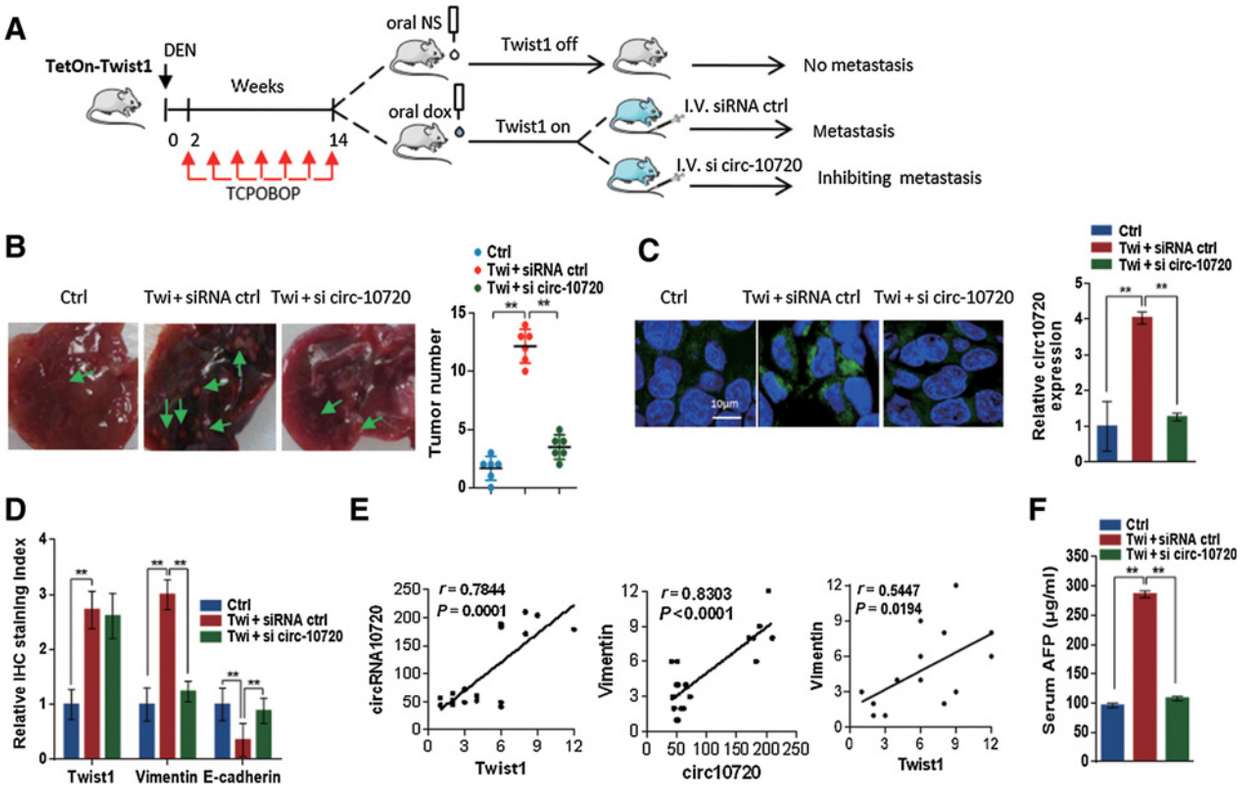

Figure 5.

circ-10720 silencing suppresses Twist1-induced tumor metastasis in a DEN-induced Tet-on-Twist1 mouse HCC model. **A,** Scheme of circ-10720 knockdown via intravenous tail injection in the DEN-induced TetOn-Twist1 mouse HCC model. **B,** Representative photos of the visible liver nodules (green arrows) in control, Twist1 + siRNA control and Twist1 + si-circ-10720 groups (left). The tumor numbers were statistically analyzed (right). Each bar represents the mean ± SD for measurements of six xenografts in each group. **, $P < 0.01$, one-way ANOVA. **C,** The expression level of circ-10720 was detected by FISH in liver tumor tissues of control, Twist1 + siRNA control, and Twist1 + si-circ-10720 groups. Each bar represents the mean ± SD for measurements of six xenografts in each group. **, $P < 0.01$, one-way ANOVA. **D,** IHC staining index of Twist1, E-cadherin, and vimentin in liver tumor tissues of control, Twist1 + siRNA control and Twist1 + si-circ-10720 groups. Each bar represents the mean ± SD for measurements of six xenografts in each group. **, $P < 0.01$, one-way ANOVA. **E,** Correlation analysis between Twist1 and circ-10720 ($P = 0.0002$), circ-10720 and vimentin ($P < 0.0001$), Twist1 and vimentin ($P = 0.0194$). The points represent the measurements of six xenografts in every group. **F,** AFP was detected by ELISA after intravenous tail injection of circ-10720. Each bar represents the mean ± SD for measurements of six xenografts in each group. **, $P < 0.01$, one-way ANOVA.

Cul2 gene are highly similar to that of the human sequence, especially the sequence of the circRNA back-splice junction site in exon 6 and exon 12. The exons 6 and 12 of human and mouse show 89% and 93% similarity, respectively. Thus, the exons 6 to 12 of murine *Cul2* also possibly form circRNA (Supplementary Fig. S7A), and the identity between has-circRNA-10720 and murine circ-10720 is 91% (Supplementary Fig. S7B). We found 32 identical bases in the back-splice junction site of the two circRNA. Thus, the siRNA of hsa-circ-10720 is also suitable for interfering with the circRNA in mice.

In TetOn-Twist1 mouse HCC model, the number of tumor nodules on the surface of the mouse livers was determined. The results showed that the mice administered doxycycline exhibited a significantly increased tumor number, and the mice injected with si-circ-10720 showed the offset results (Fig. 5B). Furthermore, we detected the circ-10720 expression level using FISH. The results showed that circ-10720 expression increased in the Twi + siRNA ctrl group and decreased to the expression level of the control group in the Twi + si-circ-10720 group (Fig. 5C). The expression level of Twist1 and vimentin in liver tumor tissues was increased in the Twi + siRNA ctrl group, whereas circ-10720 knockdown blocked the influence of Twist1 on vimentin in the Twi + si-circ-10720 group. The level of E-cadherin expression was opposite that of the expression pattern of vimentin (Fig. 5D). In addition, we analyzed the correlation between Twist1, vimentin and circ-10720 expression in liver tumor tissues. The results showed that the Twist1, circ-10720 and vimentin expression levels were positively related (Fig. 5E). The serum AFP expression levels were consistent with those of circ-10720 in control, Twi + siRNA ctrl, and Twi + si-circ-10720 groups (Fig. 5F). These data demonstrated that circ-10720 knockdown can attenuate the promotive effect on tumor growth, metastasis, and vimentin expression induced by Twist1 in a DEN–doxycycline-induced mouse HCC model.

circ-10720 serves as a biomarker of HCC

To gain further support for the role of circ-10720 in HCC development and progression and to extend our observations to a clinicopathologically relevant context, we collected 381 HCC samples and analyzed the circ-10720 expression level of using FISH. Correlation analysis between circ-10720 and vimentin

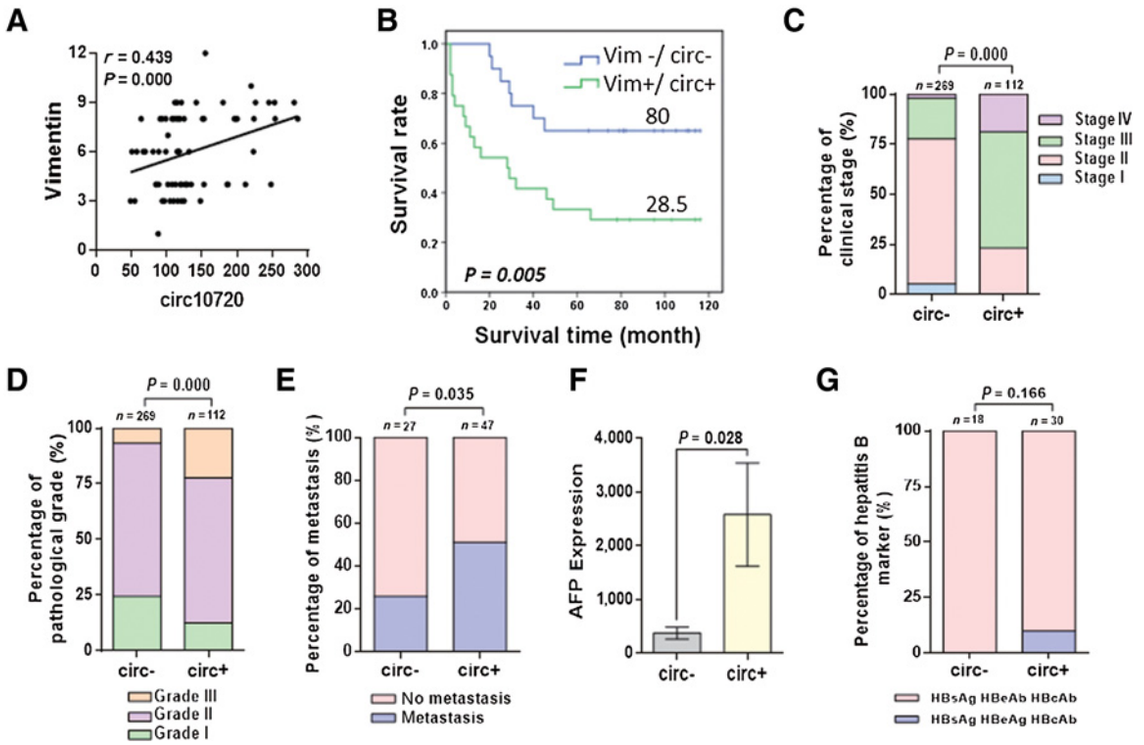

Figure 6.

circ-10720 serves as an HCC biomarker. **A,** Correlation analysis between circ-10720 and vimentin ($P = 0.000$) in 75 HCC tissues. **B,** Kaplan–Meier plots of the overall survival rate of 75 patients with HCC with vimentin/circ-10720 low (blue) or high (green) expression levels ($P = 0.005$). **C,** Percentage of each clinical stage in the circ-10720–negative and circ-10720–positive subsets ($P = 0.000$). χ^2 test. **D,** Percentage of each pathologic grade in the circ-10720–negative and circ-10720–positive subsets ($P = 0.000$). χ^2 test. **E,** Percentage of metastatic cases in the circ-10720–negative and circ-10720–positive subsets ($P = 0.035$). χ^2 test. **F,** Expression levels of AFP in the circ-10720–negative and circ-10720–positive subsets ($P = 0.028$). Student *t* test. **G,** Percentage of hepatitis B virus markers ($HBsAg^+/HBeAg^+/HBcAb^+$ and $HBsAg^+/HBeAb^+/HBcAb^+$) in the circ-10720–negative and circ-10720–positive subsets ($P = 0.166$). χ^2 test.

showed that the expression levels of circ-10720 and vimentin were positively correlated in HCC tumor tissues ($r = 0.439$, $P = 0.000$; Fig. 6A). Kaplan–Meier analysis showed that positive expression of circ-10720/vimentin was associated with shorter overall survival in 75 patients with HCC. The median survival times were 80 months and 28.5 months in the negative and positive group, respectively (Fig. 6B). Moreover, we examined the correlations between circ-10720 expression levels and clinical stage or pathologic grade in HCC cases. The percentage of clinical stages I–II was 77.7% in low expression circ-10720 HCC and 23.2% in HCC with high expression of circ-10720, whereas stage III–IV percentages were 22.3% and 76.8% in the two groups, respectively ($P = 0.000$; Fig. 6C). The percentage of pathologic grade III was 6.7% and 22.3% in low and high circ-10720–expressing groups, respectively ($P = 0.004$; Fig. 6D). The percentage of metastasis was 25.9% and 51.1% low and high circ-10720–expressing groups, respectively ($P = 0.035$; Fig. 6E). In addition, the expression level of AFP was detected in the two subsets. The level of AFP in the high circ-10720 group was significantly higher than that in the low circ-10720 group (Fig. 6F). Although the expression level of circ-10720 was not correlated with hepatitis B markers (Fig. 6G). These findings indicated that circ-10720 was correlated with poor prognosis and tumor progression, and it may serve as a potential biomarker in HCC but not in hepatitis B.

Discussion

The important role of Twist1 in EMT associated with tumor metastasis and vasculogenic mimicry formation in HCC was demonstrated in our previous study (1, 34). High Twsit1 expression presents a shorter survival time in multiple tumors, such as in breast, gastric, ovarian, and lung cancer (Kaplan–Meier plotter database, Supplementary Fig. S8A), and we confirmed in HCC (Supplementary Fig. S8B). In the current study, the ChIP-seq results showed that Twist1 binds the Cul2 promoter and a luciferase reporter assay verified that Twist1 promotes Cul2 promoter activity. Furthermore, we found that Cul2 precursor mRNA was increased and mRNA and protein levels were decreased in Twist1-overexpressing HCC cells. Therefore, Twist1 promoted Cul2 mRNA transcription but not translation. Cul2 has been predicted to be a tumor suppressor protein because of its association with the von Hippel-Lindau gene and ubiquitinated HIFα degradation (18, 19). However, it has also been reported that Cul2 is required for normal vasculogenesis and involved in cell-cycle regulation (20) and that it promotes gastric cancer progression (35, 36). In our study, we analyzed 75 HCC tissues, and the results showed that the Cul2 expression level was not significantly correlated with HCC metastasis. Therefore, we speculate that Twist1 might affect Cul2 circRNA expression and function in HCC.

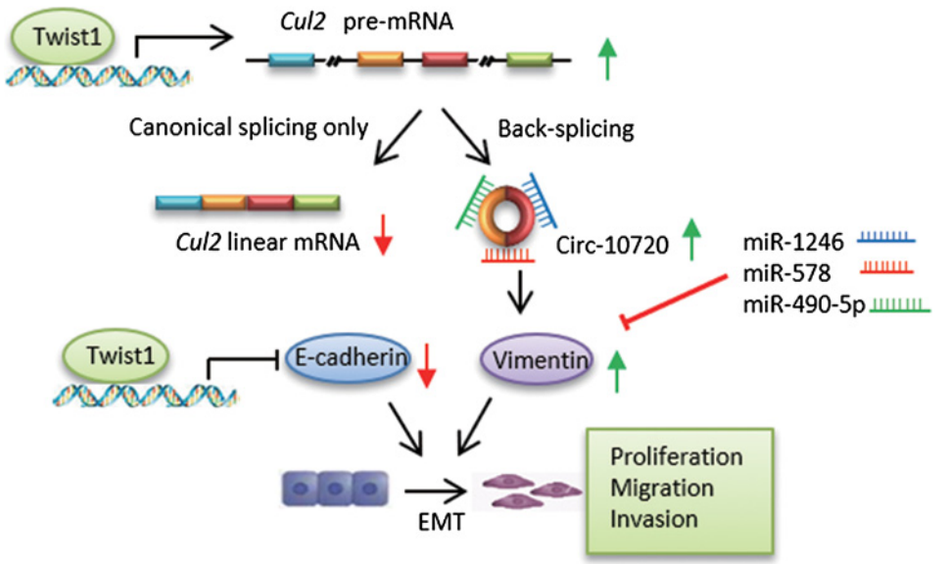

Figure 7.
The schematic diagram shows the mechanism that Twist1 regulates vimentin through circ-10720, absorbing miRNA-targeted vimentin to promote EMT in HCC.

Recently, circRNAs were rediscovered and generated by the noncanonical spliceosomal machinery (24). The heterogeneous circRNA group and their function as competing endogenous RNAs have permanently altered our perspectives on cancer, especially on carcinogenesis and cancer progression. Interestingly, a single gene locus can produce multiple circRNAs through alternative back-splicing. This alternative splicing can also expand the diversity of circRNAs, and some cassette exons are more favorably included in circRNAs than in linear mRNAs (23). Here, we found that exogenous expression of Twist1 promoted the transcription of Cul2 and Cul2-related circRNA formation. circ-10720 was associated with poor prognosis, and it promoted HCC metastasis and progression. Together, the presented evidence leads us to propose that activation of Twist and Twist-induced Cul2 circRNA are important for EMT progression.

Metastasis of tumor cells involves a complex series of biological steps that enable cells to overcome multiple barriers erected by normal tissues. Vimentin is a mesenchymal marker and responsible for maintaining cell shape and stabilizing cytoskeletal interactions. It functions as an organizer of a number of critical proteins involved in cell attachment and migration (37). In vimentin knockout mice, weak capacity fibroblasts lead to impaired wound healing in both embryonic and adult stages compared to wild-type littermates (38). Although vimentin expression has been shown to be induced by Twist1 in human cancer cells, the specific mechanism still remains unclear. In this study, we found that Twist1 regulates vimentin expression through an indirect pathway mediated by circ-10720 adsorption of miRNA. Indeed, our results indicated that circ-10720 was upregulated by Twist1 and adsorbed miRNAs targeting vimentin to release its expression at the post-transcription level. circ-10720 knockdown attenuated the effect of Twist1 on vimentin expression in HCC cells. In PDX and DEN-induced TetOn-Twist mice HCC models, the mice were treated with si-circ-10720 via intratumoral or intravenous injection. The results showed that silencing circ-10720 blocked the promotive effect of Twist1 on vimentin expression and HCC malignance and metastasis. These results demonstrated an indirect regulation mechanism of vimentin by Twist1 and indicated the important role of circRNA in EMT.

In vivo and *in vitro*, we also detected the effect of circ-10720 in promoting tumor growth and metastasis. The results of gene-expression profiling and proteomic analysis confirmed that circ-10720 upregulated genes related to tumor progression in HCC cells. Pathologic analysis the tissue samples of HCC indicated that circ-10720 was associated with poor prognosis and tumor progression, and may serve as a potential biomarker in HCC.

Although carcinogenic circ-10720 was found to mediate the regulation of vimentin by Twist1 during EMT progression in this study, we have not validated the specific regulation mechanism of Twist1 in Cul2 RNA alternative splicing and determined whether other transcriptional factors participate in the regulation process. Hence, how Twist1 regulates Cul2 circRNA formation during EMT progression in cancer still needs further investigation, and we will continue to focus on this issue in our future studies.

Altogether, we demonstrated the mechanism employed by Twist1 to regulate vimentin expression during EMT in cancer. Twist1 directly binds the *Cul2* and its promoter to contribute to aberrant formation of Cul2 circRNA, which promotes vimentin expression by sponging vimentin-targeting miRNAs (Fig. 7). circ-10720 expression was also found to promote the EMT, tumor metastasis and malignancy in HCC. Moreover, high circ-10720 levels were found to be positively correlated with Twist1 and vimentin expression in patients with HCC. Our data reveal circ-10720–mediated regulation of vimentin by Twist1 and the important role of circRNA during EMT. These findings may be useful in developing circRNA-based diagnostic and therapeutic strategies for malignant cancer.

Disclosure of Potential Conflicts of Interest

No potential conflicts of interest were disclosed.

Authors' Contributions

Conception and design: J. Meng, S. Chen, T. Sun, C. Yang
Development of methodology: J. Meng, S. Chen, J.-X. Han, X.-R. Wang, C. Zhang, T. Sun, C. Yang
Acquisition of data (provided animals, acquired and managed patients, provided facilities, etc.): J. Meng, J.-X. Han, B. Qian, X.-R. Wang, Y. Qin, W.-F. Gao, Y.-Y. Lei, W. Yan, L. Yang, C. Zhang, Y.-R. Liu, T. Sun, C. Yang

Analysis and interpretation of data (e.g., statistical analysis, biostatistics, computational analysis): J. Meng, J.-X. Han, T. Sun, C. Yang
Writing, review, and/or revision of the manuscript: J. Meng, S. Chen, T. Sun, C. Yang
Administrative, technical, or material support (i.e., reporting or organizing data, constructing databases): J. Meng, W.-L. Zhong, H. Zhang, H.-J. Liu, H.-G. Zhou, T. Sun
Study supervision: T. Sun, C. Yang

Acknowledgments

This study was supported by the National Natural Science Foundation of China (grant nos. 81572838, 81402973, and 81703581), Natural Science Foundation of Tianjin City (grant no. 15JCYBJC26400), National Science and Technology Major Project (2017ZX09306007), and Tianjin Science and Technology Project (15PTGCCX00140).

The costs of publication of this article were defrayed in part by the payment of page charges. This article must therefore be hereby marked *advertisement* in accordance with 18 U.S.C. Section 1734 solely to indicate this fact.

Received September 30, 2017; revised March 13, 2018; accepted May 16, 2018; published first May 29, 2018.

References

1. Sun T, Sun BC, Zhao XL, Zhao N, Dong XY, Che N, et al. Promotion of tumor cell metastasis and vasculogenic mimicry by way of transcription coactivation by Bcl-2 and Twist1: a study of hepatocellular carcinoma. Hepatology 2011;54:1690–706.
2. De Craene B, Berx G. Regulatory networks defining EMT during cancer initiation and progression. Nat Rev Cancer 2013;13:97–110.
3. Geiger TR, Peeper DS. Metastasis mechanisms. Biochim Biophys Acta 2009;1796:293–308.
4. Valastyan S, Weinberg RA. Tumor metastasis: molecular insights and evolving paradigms. Cell 2011;147:275–92.
5. Guo M, Ehrlicher AJ, Mahammad S, Fabich H, Jensen MH, Moore JR, et al. The role of vimentin intermediate filaments in cortical and cytoplasmic mechanics. Biophys J 2013;105:1562–8.
6. Shibue T, Weinberg RA. EMT, CSCs, and drug resistance: the mechanistic link and clinical implications. Nat Rev Clin Oncol 2017;14:611–29.
7. Eriksson JE, Dechat T, Grin B, Helfand B, Mendez M, Pallari HM, et al. Introducing intermediate filaments: from discovery to disease. J Clin Invest 2009;119:1763–71.
8. Gilles C, Polette M, Zahm JM, Tournier JM, Volders L, Foidart JM, et al. Vimentin contributes to human mammary epithelial cell migration. J Cell Sci 1999;112:4615–25.
9. Yang Y, Ye C, Wang L, An G, Tian Z, Meng L, et al. Repressor activator protein 1-promoted colorectal cell migration is associated with the regulation of Vimentin. Tumour Biol 2017;39:1010428317695034.
10. Mendez MG, Kojima S, Goldman RD. Vimentin induces changes in cell shape, motility, and adhesion during the epithelial to mesenchymal transition. FASEB J 2010;24:1838–51.
11. Salmon M, Zehner ZE. The transcriptional repressor ZBP-89 and the lack of Sp1/Sp3, c-Jun and Stat3 are important for the down-regulation of the vimentin gene during C2C12 myogenesis. Differentiation 2009;77:492–504.
12. Izmailova ES, Wieczorek E, Perkins EB, Zehner ZE. A GC-box is required for expression of the human vimentin gene. Gene 1999;235:69–75.
13. Izmailova ES, Snyder SR, Zehner ZE. A Stat1alpha factor regulates the expression of the human vimentin gene by IFN-gamma. J Interferon Cytokine Res 2000;20:13–20.
14. Wu Y, Diab I, Zhang X, Izmailova ES, Zehner ZE. Stat3 enhances vimentin gene expression by binding to the antisilencer element and interacting with the repressor protein, ZBP-89. Oncogene 2004;23:168–78.
15. Izmailova ES, Zehner ZE. An antisilencer element is involved in the transcriptional regulation of the human vimentin gene. Gene 1999;230:111–20.
16. Virtakoivu R, Mai A, Mattila E, De Franceschi N, Imanishi SY, Corthals G, et al. Vimentin-ERK signaling uncouples slug gene regulatory function. Cancer Res 2015;75:2349–62.
17. Zhang XD, Dong XQ, Xu JL, Chen SC, Sun Z. Hypoxia promotes epithelial-mesenchymal transition of hepatocellular carcinoma cells via inducing Twist1 expression. Eur Rev Med Pharmacol Sci 2017;21:3061–8.
18. Cai W, Yang H. The structure and regulation of Cullin 2 based E3 ubiquitin ligases and their biological functions. Cell Div 2016;11:7.
19. Petroski MD, Deshaies RJ. Function and regulation of cullin-RING ubiquitin ligases. Nat Rev Mol Cell Biol 2005;6:9–20.
20. Maeda Y, Suzuki T, Pan X, Chen G, Pan S, Bartman T, et al. CUL2 is required for the activity of hypoxia-inducible factor and vasculogenesis. J Biol Chem 2008;283:16084–92.
21. Cocquerelle C, Mascrez B, Hetuin D, Bailleul B. Mis-splicing yields circular RNA molecules. FASEB J 1993;7:155–60.
22. Conn SJ, Pillman KA, Toubia J, Conn VM, Salmanidis M, Phillips CA, et al. The RNA binding protein quaking regulates formation of circRNAs. Cell 2015;160:1125–34.
23. Zhang XO, Dong R, Zhang Y, Zhang JL, Luo Z, Zhang J, et al. Diverse alternative back-splicing and alternative splicing landscape of circular RNAs. Genome Res 2016;26:1277–87.
24. Sibley CR, Blazquez L, Ule J. Lessons from non-canonical splicing. Nat Rev Genet 2016;17:407–21.
25. Jeck WR, Sharpless NE. Detecting and characterizing circular RNAs. Nat Biotechnol 2014;32:453–61.
26. Chen LL. The biogenesis and emerging roles of circular RNAs. Nat Rev Mol Cell Biol 2016;17:205–11.
27. Ashwal-Fluss R, Meyer M, Pamudurti NR, Ivanov A, Bartok O, Hanan M, et al. circRNA biogenesis competes with pre-mRNA splicing. Mol Cell 2014;56:55–66.
28. Kim HY, Kim J, Ha Thi HT, Bang OS, Lee WS, Hong S. Evaluation of anti-tumorigenic activity of BP3B against colon cancer with patient-derived tumor xenograft model. BMC Complement Altern Med 2016;16:473.
29. Tsai JH, Donaher JL, Murphy DA, Chau S, Yang J. Spatiotemporal regulation of epithelial-mesenchymal transition is essential for squamous cell carcinoma metastasis. Cancer Cell 2012;22:725–36.
30. Beard C, Hochedlinger K, Plath K, Wutz A, Jaenisch R. Efficient method to generate single-copy transgenic mice by site-specific integration in embryonic stem cells. Genesis 2006;44:23–8.
31. Li Z, Tuteja G, Schug J, Kaestner KH. Foxa1 and Foxa2 are essential for sexual dimorphism in liver cancer. Cell 2012;148:72–83.
32. Cai CM, Xiao X, Wu BH, Wei BF, Han ZG. Targeting endogenous DLK1 exerts antitumor effect on hepatocellular carcinoma through initiating cell differentiation. Oncotarget 2016;7:71466–76.
33. Meng J, Liu Y, Han J, Tan Q, Chen S, Qiao K, et al. Hsp90beta promoted endothelial cell-dependent tumor angiogenesis in hepatocellular carcinoma. Mol Cancer 2017;16:72.
34. Sun T, Zhao N, Zhao XL, Gu Q, Zhang SW, Che N, et al. Expression and functional significance of Twist1 in hepatocellular carcinoma: its role in vasculogenic mimicry. Hepatology 2010;51:545–56.
35. Chen P, Yao GD. The role of cullin proteins in gastric cancer. Tumour Biol 2016;37:29–37.
36. Su Y, Ni Z, Wang G, Cui J, Wei C, Wang J, et al. Aberrant expression of microRNAs in gastric cancer and biological significance of miR-574–3p. Int Immunopharmacol 2012;13:468–75.
37. Kidd ME, Shumaker DK, Ridge KM. The role of vimentin intermediate filaments in the progression of lung cancer. Am J Respir Cell Mol Biol 2014;50:1–6.
38. Eckes B, Colucci-Guyon E, Smola H, Nodder S, Babinet C, Krieg T, et al. Impaired wound healing in embryonic and adult mice lacking vimentin. J Cell Sci 2000;113:2455–62.